IEEE Access
Multidisciplinary ⋮ Rapid Review ⋮ Open Access Journal

Received 1 July 2022, accepted 22 August 2022, date of publication 29 August 2022, date of current version 16 September 2022.

Digital Object Identifier 10.1109/ACCESS.2022.3202920

RESEARCH ARTICLE

A Numerical Model to Evaluate the HVAC Power Demand of Electric Vehicles

AMBARISH KULKARNI[1], (Member, IEEE), GERRIT BRANDES[2], (Student Member, IEEE), AKHLAQUR RAHMAN[3], (Senior Member, IEEE), AND SHUVA PAUL[4], (Member, IEEE)

[1]Department of Mechanical Engineering and Product Design Engineering, Swinburne University of Technology, Hawthorn, VIC 3122, Australia
[2]Department of Vehicle Drives and Transmissions, Technische Universitat Braunschweig, Braunschweig, 38106 Niedersachsen, Germany
[3]Engineering Institute of Technology, West Perth, WA 6872, Australia
[4]Georgia Institute of Technology, Electrical and Computer Engineering, Atlanta, GA 30332, USA

Corresponding author: Ambarish Kulkarni (ambarishkulkarni@swin.edu.au)

ABSTRACT There has been a significant increase in demand for electric vehicles (EVs) in recent times due to existing environmental situations and an ever rising concern for energy. Due to the electrification of transportation and customer requirement, there is a concentrated focus on vehicle performance of EVs as a prime criterion. Amongst performances, range anxiety caused by the poor energy densities of the batteries, is one of the major drawbacks in these EVs. Possible mitigation for these scenarios includes, increasing the battery capacity, using dual energy sources and/or optimising the energy demands. After the propulsion system, auxiliary systems have an immense impact on the energy demands, the most significant being the heating ventilation and air-conditioning (HVAC) unit. With that in mind, this study develops a thermal model to analyse the required HVAC power for varying vehicle specifications. To benefit from the simplicity and versatility of one-dimensional ($1D$) numerical models, the passenger cabin of a city bus was modelled in Matlab Simulink. Next, empirical relations were employed to take external convection, wall conduction, solar radiation and passenger heat generation into account. Additionally, the influence of the forced internal convection of the conditioned air flow in the passenger cabin was modelled and analysed in a three-dimensional ($3D$) CFD simulation and then transferred into the $1D$ model. The results of the CFD simulation were also used to validate the $1D$ model in early stages of development. The model was then used to examine the effect of insulation and reflectivity optimization on the HVAC power consumption at different vehicle speeds. To the best of our knowledge, the model developed in this paper can be used to evaluate the required HVAC power, thus maintaining a required cabin temperature for various heavy vehicle specifications as well as boundary conditions.

INDEX TERMS Heating, ventilation and air conditioning, vehicle HVAC, heavy duty electric vehicle, bus cabin model, thermal modeling.

I. INTRODUCTION

Due to the impending shortage of fossil fuels and increasingly stricter exhaust regulations around the globe, the global annual electric vehicles (EV) sales has increased by the factor of ten from 134 thousand in 2012 (0.07% vehicle market share) to 1.281 million in 2017 (1.34% market share) [1]. The increasing demand for electric drivetrains [2], [3] applies not only to private transportation but also to public transport as well. While the majority of trains are already electrically driven, most passenger buses are still equipped with conventional combustion engines. One of the factors is the limited range and in turn the versatility of the electric drive train [4]. While the energy consumption of auxiliary equipment marginally influences the range of conventional vehicles, it is critical in the scenario of EVs. While several studies have focused on the the planning/optimization of renewable integration (e.g., [5], [6], [7]) in order to accommodate Electric Vehicle, another aspect that needs to be critically addressed fpr this given scenario is the need/desire

The associate editor coordinating the review of this manuscript and approving it for publication was Chandan Kumar.

to reduce the power consumption of the auxiliary systems. In this context, the most significant is the heating, ventilation and air conditioning (HVAC) system which can reduce the cruising range of battery electric vehicles (BEVs) by up to 22% depending on drive cycle and climate conditions [8], [9], [10], [11], [12]. In particular due to the disadvantageous initial cabin temperatures (i.e. after parking in the sun) the range can even be reduced by 68% [13].

One key element in achieving the HVAC power reduction is avoiding the use of an oversized HVAC unit in the first place. The second approach includes the thermal optimization of the vehicle itself, by implementing measures such as increasing the use of insulation materials, reflective paints, etc. To include these two considerations at an early state stage in the design process of a new vehicle and to avoid high costs for prototyping and testing, numerical modelling and simulation of the vehicle and thereby predicting its thermal performance is necessary. The thermal model introduced in this study aims to serve the purpose mentioned above. It can be used to either identify the necessary HVAC system capacity for new vehicle designs or to assess the efficacy of different optimization approaches to reduce the HVAC power requirement. A similar thermal model was developed by Jefferies *et al.* to analyse the life cycle costs of different HVAC systems for a city bus in middle European climate [14]. A one-dimensional (1D) energy balance model of the bus passenger cabin was used to evaluate heating and cooling demands for the HVAC unit. The cabin was modelled as one volume with uniform temperature distribution. All heat transfer processes and thermal loads were based on analytic relations. A detailed HVAC unit model (including vapor compression cycle, electric resistance heater, etc.) was used to evaluate the power demand. Paulke *et al.* [15] conducted a three-dimensional (3*D*) CFD simulation to predict passenger comfort in a city bus, and the HVAC power demand to enforce a constant cabin temperature based on various boundary conditions was successfully evaluated. CFD simulations have also been used by Patil *et al.* [16] to validate a 1*D* solar heating model of a standing car and by Zhang *et al.* [17] to predict the temperature and airflow distribution in the driver cabin of a truck. Kusiak *et al.* [18] proposed a data-driven approach to model and optimize the HVAC energy consumption of buildings by using data-mining and particle swarm optimization algorithms, thus avoiding detailed modeling of the physical principles. Perez-Lombard *et al.* [19] introduced an energy map for building HVAC systems based on energy balance to identify the energy-saving potentials at different stages of the HVAC energy chain. There have also been studies performed by Jari *et al.*, [20] as well as Irfan *et al.*, [21] who focused on energy demand prediction in different operating conditions using surrogate and regression-based models, respectively. Additionally, Amier and Fangming [19] recently provided an overview of different numerical models for EV energy demand predictions with a focus on equivalent circuit models.

Compared to the current state-of-the-art, the 1*D* model described in this paper differs from the previously mentioned approaches, as it utilizes a combination of analytical relations and CFD inferred heat transfer coefficients to model airflow and heat flux through the passenger cabin, the air ducts, and the HVAC unit, thus combining the accuracy of a CFD simulation with the versatility and reduced computing time of a one-dimensional model. As the duct and cabin volumes are divided into separate regions and the positions of air vents are specified, the non-uniform temperature distribution within the volumes is taken into account. The overall contribution of the paper are:

1) Exploring the novel technique of coupling 3D CFD simulations with 1D simulations to achieve results that are accurate and reliable while avoiding reliance on costly physical testing and developing a modular math based system model.
2) Developing methods and tool by relying mainly on a 1D model as the main solver and being used effectively as a parametric tool to perform quick performance and efficiency studies for various factors influencing performance of EV and HVAC systems such as human factors, environmental factors, material properties, vehicle operating conditions etc.
3) Generating a 1D tool capable of providing accurate reliable results based only on preliminary design and verification parameters, thus enabling the math based tool to be easily adopted for application across a wide range of systems and domain.
4) The main contribution of the tool is its ability for faster turn around of design, optimisation and verification tasks and it's agility to be applied across a wide range of domains due to its inherent simple block and math-based architecture.

The rest of the paper is organized as follows.At first, this paper deals with the fundamentals of vehicle HVAC systems in general and bus HVAC systems in particular. In the next step, the method to infer heat transfer coefficients (HTCs) from a CFD simulation and the corresponding CFD model are addressed. Next, the paper discusses the implementation of the 1*D* numerical model. Finally, the developed 1*D* model is used to evaluate the sensitivity of the bus HVAC power demand concerning two optimization strategies.

II. VEHICLE HVAC SYSTEM FUNDAMENTALS

Vehicle HVAC systems [22] serve to provide a comfortable cabin climate for the passengers regardless of the ambient conditions. To maintain this climate, the unit has to compensate any heat and humidity loads on the cabin, i.e. it has to dehumidify and heat/cool the cabin air. The cabin air is therefore dragged into the return air inlet of the HVAC unit. The conditioned air is then distributed from the HVAC unit via a duct system into the cabin. Some of the thermal loads enter the vehicle via its boundary surfaces (roof, floor, walls and windows) without mass exchange. Others come with the mass exchange between cabin and ambience due to leakage and open doors or are emitted by the passengers. The following list of all processes involved in loading the cabin air is visualized in Figure 10:

- Solar heating of external boundary surfaces
- Radiation heat exchange between external boundary surfaces and ambient objects
- External convection heat exchange between vehicle body panels and ambient air
- Internal convection heat exchange between vehicle body panels and cabin air
- Internal convection heat exchange between internal masses (seats, etc.) and cabin air
- Internal conduction and radiation heat exchange between vehicle parts (engine, exhaust, etc.) and boundary surfaces
- Passenger heat and humidity loads (acting directly on cabin air)
- Air exchange between cabin and ambience due to leakage, open doors and fresh air intake (heat load and humidity load)

For their complexity the humidity load as well as the mass exchange between cabin and ambient air were omitted in the developed model but are desired to be taken into account by further research. The engine heat load is neglected due to low waste heat production by the electric power train in the analysed vehicle. The internal convection [23] was addressed in the $1D$ model by implementing HTC values gained from the CFD analysis, as this heat transfer mechanism depends on the geometries and vent positions of the analysed vehicle. All other heat transfer processes were included in form of analytical relations provided in the standard literature (e.g. [24], [25]). Details on the implementation in the $1D$ model can be found in later in the paper. Different technologies for vehicle HVAC systems are available. Cooling and dehumidification is usually achieved by utilizing a vapour compression cycle. This system can theoretically also provide a heating function (reversed cycle heat pump). The simplest implementation of a vapour compression cycle is displayed shown in Figure 1.

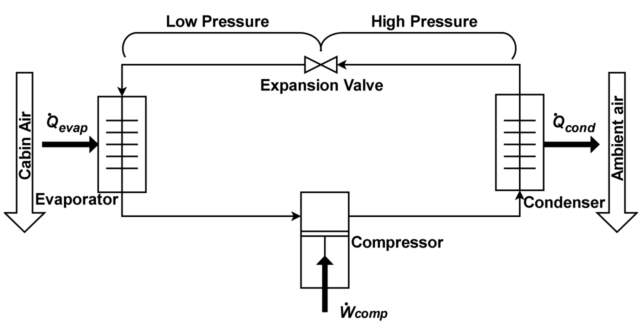

FIGURE 1. Components and heat flux in a simple ideal vapour compression cycle.

Details on fundamentals, calculation methods and design of vapour compression cycles can be found in corresponding literature (e.g. [26], [27]). Other methods to heat the cabin air include electrical resistance heaters and engine cooling cycle heaters which use the waste heat of a combustion engine. The latter are optionally equipped with additional auxiliary heaters and are generally not applicable for electric buses, as the electric power-train does not provide sufficient quantities of waste heat. Furthermore, it is not desired to eliminate the zero local-emission advantage of electric vehicles by implementing fuel powered auxiliary heaters. Both the electrical resistance heaters and the engine cooling cycle heaters can be directly mounted in the passenger cabin as convectors or be implemented in the HVAC system. The HVAC system implemented in the $1D$ model is the "$X-1000E''$ unit manufactured by Thermo King Cooperation, a roof mounted vapour compression system with electric resistance heating functionality. The technical specifications of this unit are to be found in Table 1.

TABLE 1. Technical data of the implemented HVAC unit.

Measure	Value
Max. evaporator air flow, $\dot{V}_{\max}$	$5100\ m^3/h$
Max. cooling capacity, $\dot{Q}_{cool,\max}$	$24\ kW$
Max. heating capacity, $\dot{Q}_{heat,\max}$	$10\ kW$
COP of vapour compression cycle, COP_{cool}	2.1
COP of PTC heater, COP_{heat}	1.0

The analysed vehicle is an electric 12.5 metre city bus. The geometry is based on the "*XDi*12.5 *Metre*" bus of Bustech Pty Ltd.

III. EVALUATION OF INTERNAL HTCS FROM CFD SIMULATION

The main cabin air heat load consists of convection heat exchange with the vehicle body panels. The resulting heat flux generally depends on the fluid properties (in this case air) and the flow situation of the fluid. The cabin air flow is actively influenced by the conditioned air entering from the vents, leading to forced convection heat transfer. Analytical relations for convection are only available for simple fluid flow scenarios (e.g. parallel flow over a flat plane). As the flow field in the analysed bus passenger cabin is a complex scenario, a steady state CFD simulation was conducted to evaluate the heat transfer. Therefore, a simplified $3D$ CAD model of the XDi bus was created and meshed using tetrahedral cells. The three main volume regions (cabin, left-hand side duct and right-hand side duct) were each divided in seven subregions along the length of the bus to address non-uniform temperature distribution within the volumes. A schematic of the used geometry is shown in Figure 2.

After the required mesh quality (maximum skewness $<$ 0.95) was achieved, boundary conditions (as specified in Table 2) and physical models (as specified in Table 3) were applied to the CFD model.

Constant temperature boundary conditions were applied to all cabin surfaces. The temperature of the air flowing into the cabin was also set as constant. From the steady state solution

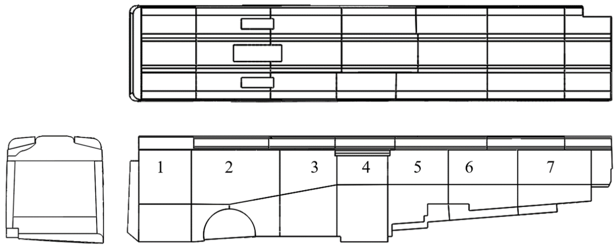

FIGURE 2. Vehicle geometry used, with numbered sub-regions.

TABLE 2. Boundary conditions for the CFD simulation.

Surface Groups	Selected Boundary Type	Fluid Specification	Thermal Specification, $T(K)$
Inlets	velocity - inlet	$v = 3.53m/s$ (const.)	291.15
Outlet	pressure-outlet	$p = 1e05Pa$ (const.)	300.00
Roofs	wall	–	333.15
Walls	wall	–	323.15
Windows	wall	–	323.15
Floors	wall	–	313.15
Seats	wall	–	313.15

TABLE 3. Physical models selected for CFD simulation.

Model	Option
Multiphase	Off
Energy	On
Viscous (Turbulence)	Realizable k-e, Standard Wall Function
Radiation	Off
Heat Exchanger	Off
Species	Off
Discrete Phase	Off
Solidification and Melting	Off
Acoustics	Off
Eulerian Wall Film	Off
Electric Potential	Off

the heat flow $\dot{Q}_{CFD}$, wall surface temperature T_w, average adjacent cell zone temperature $T_{(av, adj)}$ and surface area A were evaluated for each surface group. Corresponding HTC values were calculated using the following equation:

$$\alpha_{CFD} = \frac{\dot{Q}_{CFD}}{A \cdot \left(T_w - T_{av,a\ dj}\right)} \tag{1}$$

These HTC values were implemented in the $1D$ model to replicate the heat transfer characteristics from the CFD analysis. The air mass flow and corresponding pressure drop for each vent group were also calculated for implementation in the $1D$ model. Additionally, the HVAC return air temperature and the inlet and outlet energy flux were evaluated for validation of the $1D$ model at a later stage.

IV. ONE-DIMENSIONAL VEHICLE MODEL

The one dimensional model was created using the graphical modelling language Matlab Simulink and the Simscape extension. The Matlab script programming language was used to define all model parameters. To begin with, a simple model of the system was created with an aim to reproduce CFD results by validating the transfer of physical behaviour from the 3D model to the 1D model. This model was further extended to represent realistic thermal behaviour. The model contains parameter and logic values. Parameter values represent geometric parameters, material properties and physical properties of the system and logic values represent the systems behaviour. Geometric properties were inferred from the CAD model and the CFD mesh model, material properties were based on the material used in the construction of the bus and physical parameters such as HTCs, pressure drops, mass flow rates, velocities, temperatures are deduced from the 3D CFD model. The same boundary conditions as used in the CFD model (Table 2) were implemented in the $1D$ model to validate its response and behaviour. The physical processes along with the underlying analytical relation form the logic values which were built into the Simscape model.

Subsystem models were created in Simulink to represent the physical subsystems such as the cabin, HVAC ducts and the bus wall. The Simulink model components are allocated with suitable parametric values in the Matlab workspace and not hardcoded into the components themselves to preserve the clarity of the model. Figure 3 shows the interconnected subsystem models for the different cabin compartments in the Simulink model. Multiple such interconnections were built to represent the various volumes into which the cabin is sub-divided.

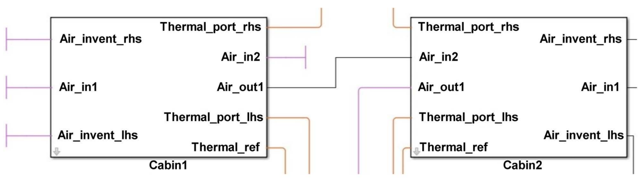

FIGURE 3. Connection between cabin subsystems.

Figure 4 shows the different logic blocks used in the Simulink model to represent the various aspects of the cabin subsystems behaviour. Interaction between subsystem components like walls, windows, floor and ducts with air volumes in cabin in the form f air flow and heat flow were modelled.

A similar subsystem model was developed to represent the HVAC ducts and another subsystem model was developed to model the air volume contained in both the ducts and the cabin subsystems to provide a connection between the heat flow and the air flow. The subsystems are shown in Figure 5 and 6.

The resulting temperature difference between inlet and outlet boundary was evaluated as $12.59K$ after time convergence for the $1D$ model and $12.50K$ for the $3D$ model. Figure 7, 8 and 9 compare the $1D$ model and CFD model predictions for heat flux and mass flows and it can be seen that there is good correlation between the results of the two models.

After successful validation the $1D$ model was further enhanced to implement more realistic thermal behaviour. Enhancements were achieved by implementing walls with

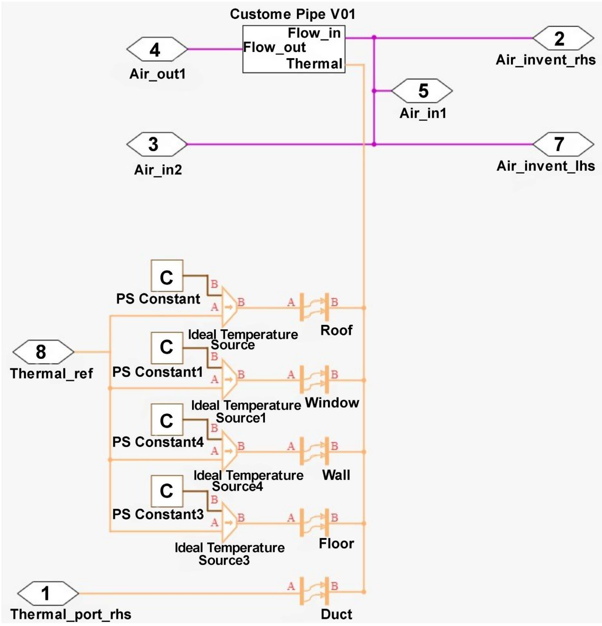

FIGURE 4. Simulink model representing the cabin subsystem behaviour.

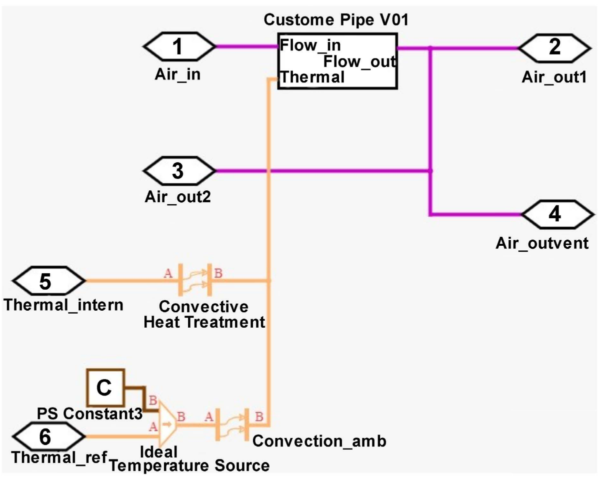

FIGURE 5. Duct subsystem model.

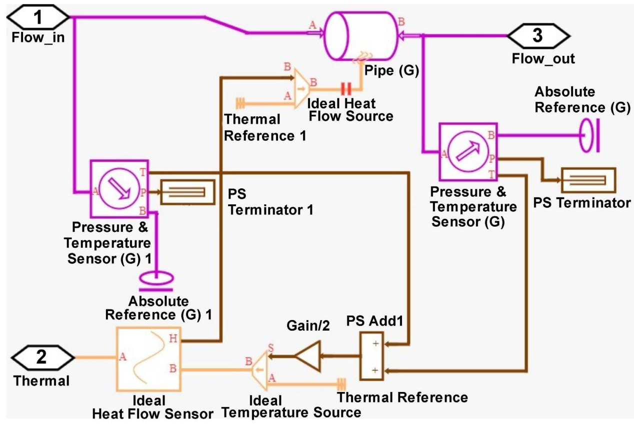

FIGURE 6. Custom pipe subsystem model.

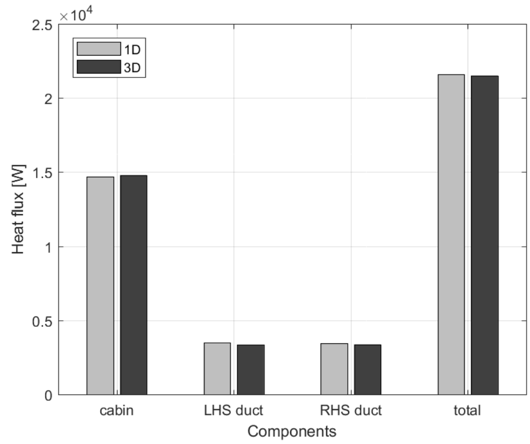

FIGURE 7. Validation results: heat flux from ambience into main vehicle components.

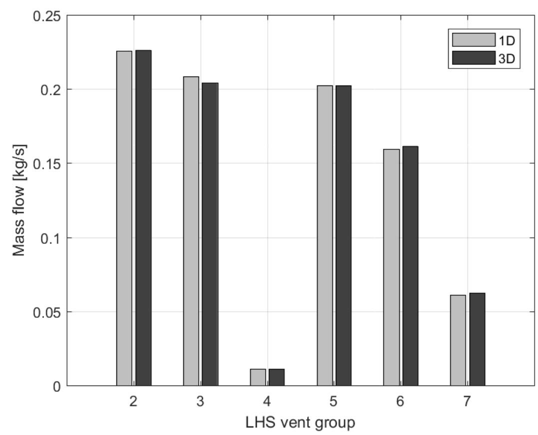

FIGURE 8. Validation results: mass flow through vent groups on LHS.

thicknesses, mass and material properties, external convective and radiation heat transfer, internal masses in the form of seats and passenger heat loads. Model enhancements led to the creation of more models for external convection subsystem, passenger subsystem, wall subsystem and a HVAC unit subsystem. All addressed physical processes, the methods of implementation and the underlying analytical relations are displayed in Table 4. A schematic visualization of all included processes is displayed in Figure 10.

The intended model use case where the parameter and logic values were combined, is visualized in the user-model interaction diagram in Figure 11. Despite the comprehensive enhancements, several simplifying assumptions are included in the $1D$ model. The assumptions made in the development of the model are categorized as the ones requiring further research and those that are considered to have negligible influence on the overall results and hence can be neglected.

TABLE 4. Implementation of physical processes in the 1D model.

Physical Process	Implementation	Analytical Relation	Equation Number	Origin of Equation
Solar heating	Simscape block	$R_G = R_{DN}\cos(\zeta - \xi) + R_{DIFF}$	Eq. 2	Equation for heat transfer by solar irradiation
Radiation	Simscape block	$\dot{Q}_{w,amb} = \varepsilon_w \sigma A \left(T_w^4 - T_{amb}^4\right)$	Eq. 3	Equation for heat transfer by radiation
Convection	General	$\dot{Q}_{w,f} = \alpha A \left(T_w - T_f\right)$	Eq. 4	Equation for heat transfer by convection
External HTC	Matlab function	$\alpha = \lambda Nu/L$	Eq. 5	Equation for convective heat transfer coefficient
Internal HTC	Simscape block	$\alpha = \alpha_{CFD}$	Eq. 6	Equation for substituting in Simscape
Conduction	Simscape block	$\dot{Q}_{1,2} = \lambda A \left(T_1 - T_2\right)/d$	Eq. 7	Equation for heat transfer by conduction
Passenger heat load	Matlab function	$\dot{Q}_{\text{pass}} = \left(166 - 3.8 \cdot \frac{\vartheta_{\text{ref}}}{[K]}\right)[W]$ $\vartheta_{ref} = \begin{cases} 16^\circ\text{C for } \vartheta_{cabin} \leq 16^\circ\text{C} \\ \vartheta_{cabin} \text{ for } 16^\circ\text{C} < \vartheta_{\text{cabin}} < 28^\circ\text{C} \\ 28^\circ\text{C for } \vartheta_{\text{cabin}} \geq 28^\circ\text{C} \end{cases}$	Eq. 8	From literature review [14]

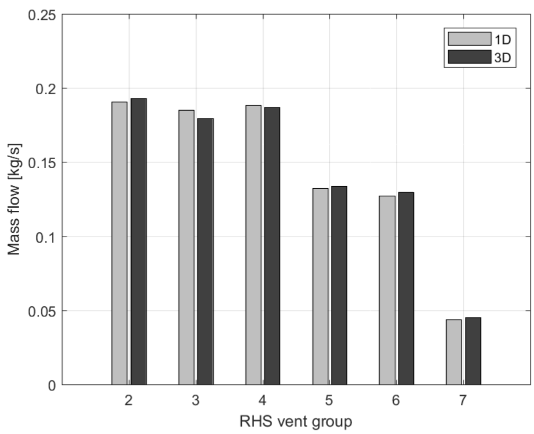

FIGURE 9. Validation results: mass flow through vent groups on RHS.

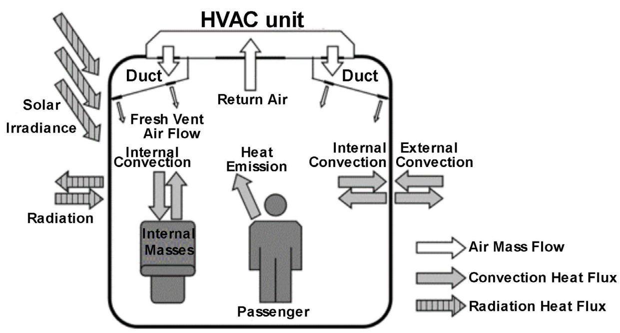

FIGURE 10. Physical processes included in the 1D model (schematic).

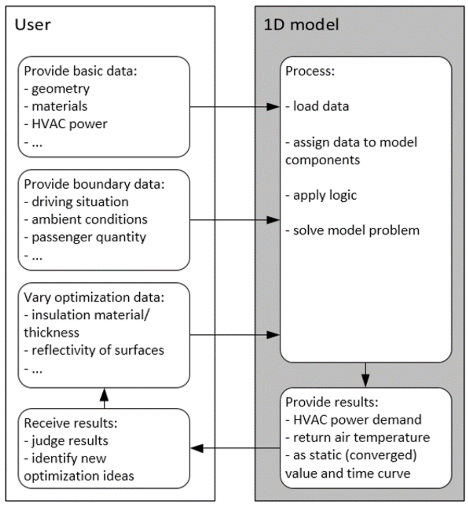

FIGURE 11. Intended user-model interaction.

The assumptions are listed below:

- HVAC unit modelled as heat flow extraction from recycling air. No detailed model of the vapour compression cycle. Additionally, the controller parameters not equal to real system.
- Analytical relations for the external heat transfer processes. External vehicle shape assumed as cuboid. Influence of assumption depending on real vehicle shape.
- Internal convection HTCs only specified for maximum HVAC air flow. Variation in air flow with time has not been considered.
- Total vehicle volume assumed to be fully enclosed. No air leakage. No air exchange for open doors. No fresh air intake in HVAC unit.
- Only seats, roof, floor, windows and walls addressed as internal masses. Other vehicle equipment (grab handles, etc.) neglected.
- Heat emission of the drive train neglected.
- Humidity load on cabin air not taken into account.

Negligible influence on results:

- Solar irradiance load evenly distributed on all vehicle sides. Real driving orientation and sun position not taken into account.
- Walls assumed to be flat and uniform. Influence of bus frame construction on wall conductivity neglected
- Passenger heat emission solely dependent on individual cabin region temperature. Fluid flow situation around passenger resulting in convective heat transfer not addressed.

After enhancement, the $1D$ model was used to simulate a basic case to investigate its general behaviour. Therefore the time curves for air mass flow, return air temperature, controller difference (temperature difference between return

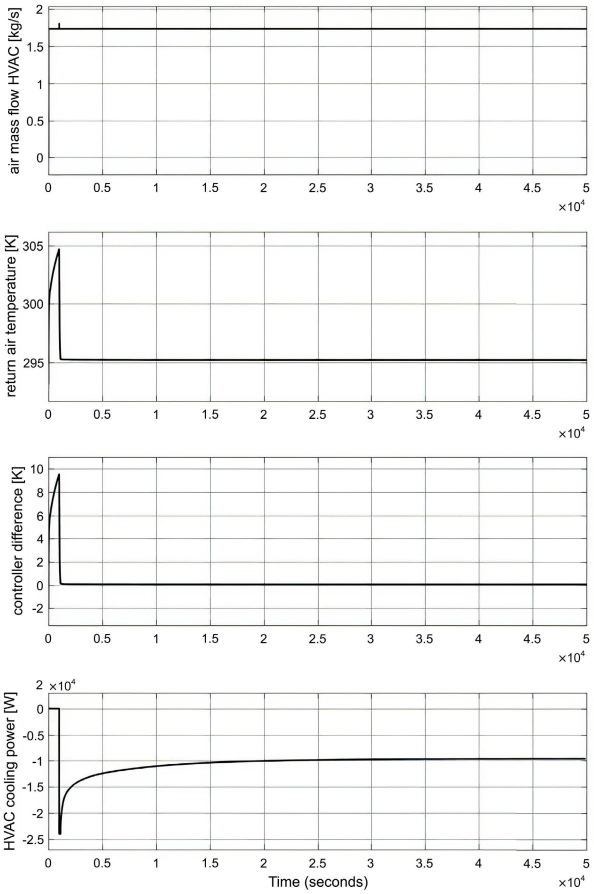

FIGURE 12. Time curves of enhanced model results for $v = 0\ km/h$.

TABLE 5. Model parameters for basic case simulation.

Model Parameter	Value
Desired cabin temperature	$22\ ^\circ C = 295.15\ K$
HVAC unit specifications	see Table 1
Simulation time	$50000\ s$
HVAC start time	$1000\ s$
Wall insulation	polystyrene, $38\ mm$
Wall cover	aluminium, $2 \times 3\ mm$
Roof insulation	polystyrene, $38mm$
Roof cover	aluminium, $2 \times 3\ mm$
Floor insulation	fiber glass composite, $15\ mm$
Floor cover	venyl, $3\ mm$
Window	float glass, $4\ mm$
Exterior surfaces	white lacquer
Ambient air temperature	$28.7°C = 301.85K$
Solar irradiance (direct normal)	$761.5W$
Solar irradiance (diffuse)	$259.13W$
Vehicle velocity	$[0, 30, 50, 80]km/h$

air and desired cabin temperature) and the HVAC heating/cooling power were evaluated (see Figure 12) for the model specifications detailed in Table 5.

The specified solar radiation loads and ambient air temperature were evaluated for an average day in Melbourne, Australia. As can seen from the time curves, the mass flow converged almost immediately. At the beginning, the return air temperature rose continuously, while the HVAC power remained zero. This process represents the heating of the bus components from the initial temperatures due to the disabled HVAC unit. At $t = 1000s$ the HVAC unit controller was switched on, thus leading the HVAC power to rise to its negative maximum of 24 kW. In the following time the return air temperature was controlled by the HVAC unit to meet the desired cabin temperature. After approximately 35000 seconds the influence of the preheating had subsided, so that a static cooling power of 9.607 kW was required to maintain the return air temperature on the desired level. The qualitative course of the displayed curves appears realistic. The simulations were also the basis for the sensitivity analysis conducted later.

V. SENSITIVITY ANALYSIS

To reduce the static HVAC energy demand while maintaining a constant cabin temperature, three basic approaches will be applicable:

- Improve insulation braess2011vieweg [28]
- Improve reflectivity (i.e. reduce absorptivity) of exterior surfaces [28]
- Reduce air losses (chassis leakage, air exchange through open doors)

As air exchange between the cabin and the ambience was not included in the created $1D$ model, only the first two options were conducted. The insulation improvement can be achieved by enhancing the insulation thickness (as conducted for this analysis) or by using materials with lower thermal conductivity. Absorptivity reduction can be applied to wall surfaces by painting or coating and to window surfaces by coating or utilizing a different glass type. In order to address the insulation and absorptivity improvement, the optimization factors were introduced for both system qualities. A factor of 1.0 equals 100% of the value used in the basic case simulation. Absorptivity and insulation were both varied by 10% of the basic values. The absorptivity factor impacts exterior surfaces, i.e. roof, windows, walls and floor. The insulation factor on the other hand applies only to the insulation layer thickness in every wall thereby not changing the insulation properties of windows.

All combinations of these variations were simulated for vehicle velocities of $v = [0, 30, 50, 80]$ km/h. The resulting simulation plan with the respective predicted absolute HVAC power consumption is displayed in Table 6.

The resulting static HVAC power demand for all simulation cases are displayed over the vehicle velocity in Figure 13.

As can be seen, the HVAC power demand decreases with increasing vehicle speed. This occurs due to the rising heat transfer coefficient at the exterior vehicle surfaces for higher free stream velocities. All optimization approaches had a similar impact on the HVAC power consumption regardless of the vehicle speed.

Figure 14 to Figure 17 show the resulting HVAC power reductions for all analysed specifications. The colour of each

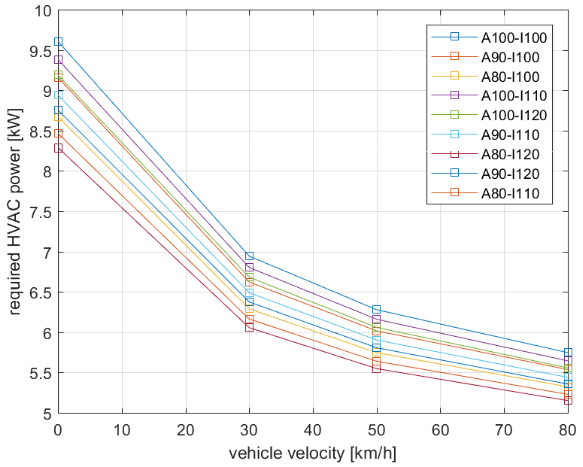

FIGURE 13. Resulting static HVAC power demand over vehicle velocity for all specifications.

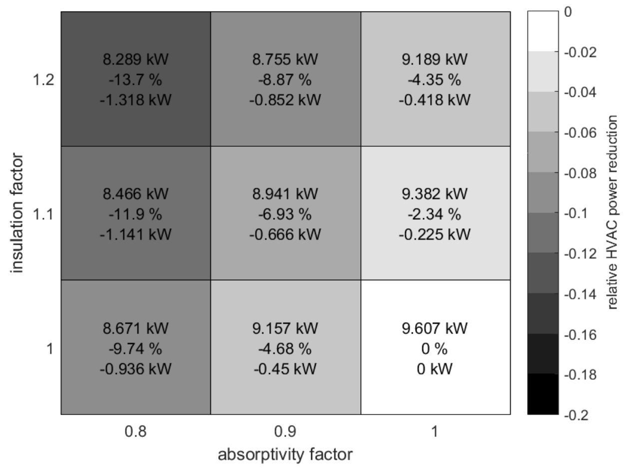

FIGURE 14. Static HVAC power demand for all specifications at v = 0 km/h.

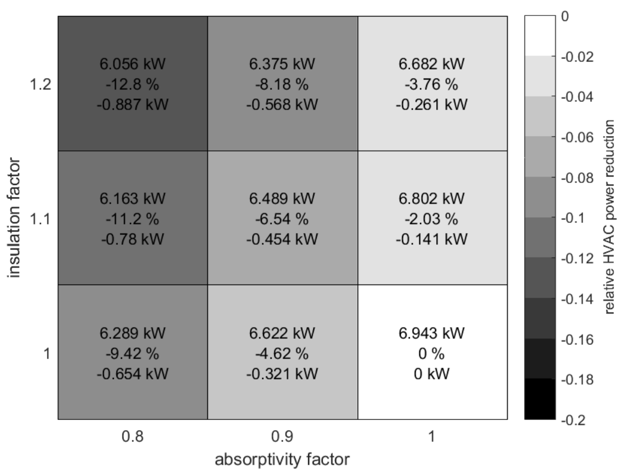

FIGURE 15. Static HVAC power demand for all specifications at v = 30 km/h.

field and of the corresponding colour scale refers to the relative power reduction. The values within each field indicate

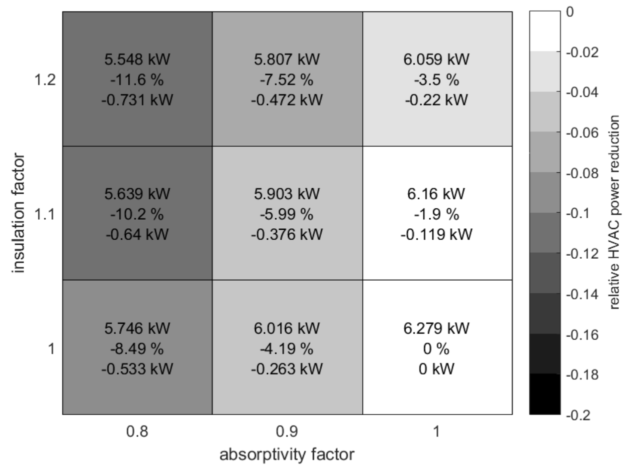

FIGURE 16. Static HVAC power demand for all specifications at v = 50 km/h.

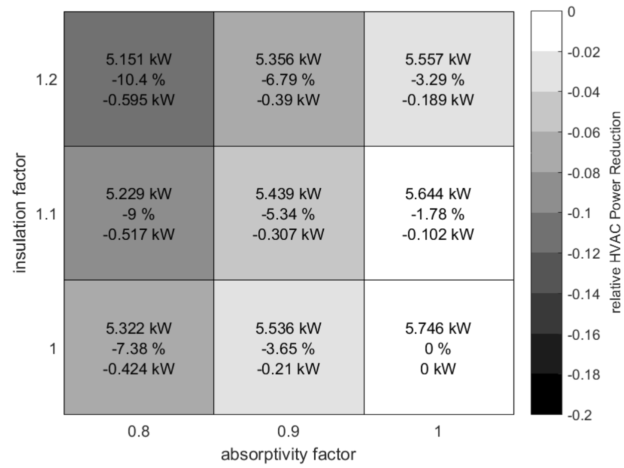

FIGURE 17. Static HVAC power demand for all specifications at v = 80 km/h.

the absolute static HVAC power demand, the achieved relative reduction (corresponding with the field colour) and the achieved absolute power reduction. All power reduction values (absolute and relative) are provided with respect to the power demand without any optimization, i.e. insulation factor = absorptivity factor = 1.0, for the specific vehicle speed. As expected the most significant power reduction occurred for the combination of maximum insulation and minimum absorptivity at all vehicle velocities. Higher relative and absolute power reductions were achieved for lower vehicle speeds. This can be lead back to the corresponding higher HVAC power demand for these driving situations.

The HVAC power demand is found to be more sensitive to the absorptivity than the insulation at all vehicle speeds. This can be traced back to the fact that the insulation factor only impacts the insulation layer thicknesses, while the absorptivity factor is applied to all exterior surfaces, including windows.

TABLE 6. Simulation plan to evaluate sensitivity for absorptivity and insulation, with absolute results.

No.	Name	Abosrptivity		Insulation		HVAC power [kW] at: (km/h)			
		90%	80%	110%	120%	0	30	50	80
0	$A100 - I100$	-	-	-	-	9.607	6.943	6.279	5.746
1	$A90 - I100$	X	-	-	-	9.157	6.622	6.016	5.536
2	$A80 - I100$	-	X	-	-	8.671	6.289	5.746	5.322
3	$A100 - I100$	-	-	X	-	9.382	6.802	6.160	5.644
4	$A100 - I120$	-	-	-	X	9.189	6.682	6.059	5.557
5	$A90 - I110$	X	-	X	-	8.941	6.489	5.903	5.439
6	$A80 - I120$	-	X	-	X	8.289	6.056	5.548	5.151
7	$A90 - I120$	X	-	-	X	8.755	6.375	5.807	5.356
8	$A80 - I110$	-	X	X	-	8.466	6.163	5.639	5.229

VI. EPILOGUE

The one-dimensional model introduced in this paper is suitable to analyse the static HVAC power demand for any vehicle specification under the limitation that the exterior vehicle shape does not significantly differ from that of a cuboid. Vehicle geometries, materials and boundary conditions can be edited manually by the user to estimate the HVAC power demand for a new vehicle, identify effective optimization strategies and gain understanding of each parameter's impact.

The conducted simulations showed that the HVAC power demand significantly depends on the vehicle velocity. Furthermore, it could be seen that for the analysed case the HVAC power is more sensitive towards the exterior surface absorptivity (Radiation factor) than the insulation thicknesses (conduction factor) at all vehicle speeds. However, this may vary for other vehicle specifications and boundary conditions. The appropriate choice of optimization strategy by the individual manufacturer depends mainly on the corresponding economic factors, i.e. increasing material and/or manufacturing prices to apply the analysed improvements. The developed model only provides an estimation of the effect of these optimizations.

In order to guarantee validity of the simulation results and the model itself, further extensive research in this domain is required. Specially, physical testing is highly encouraged to validate the current model.

Furthermore, the model requires additional enhancement to eliminate the many assumptions. This mainly includes accounting air humidity, accurate HVAC unit modelling, addressing air exchange and analysing internal heat transfer for different HVAC air mass flows.

REFERENCES

[1] R. Irle. *Global Plug-in Vehicle Sales Reached Over 3.2 Million in 2020*. Accessed: 2018. [Online]. Available: https://www.ev-volumes.com/country/total-world-plug-in-vehicle-volumes

[2] G. De Filippis, B. Lenzo, A. Sorniotti, P. Gruber, and W. De Nijs, "Energy-efficient torque-vectoring control of electric vehicles with multiple drivetrains," *IEEE Trans. Veh. Technol.*, vol. 67, no. 6, pp. 4702–4715, Jun. 2018.

[3] J. Ruan and Q. Song, "A novel dual-motor two-speed direct drive battery electric vehicle drivetrain," *IEEE Access*, vol. 7, pp. 54330–54342, 2019.

[4] M. Vafaeipour, M. El Baghdadi, F. Verbelen, P. Sergeant, J. Van Mierlo, and O. Hegazy, "Experimental implementation of power-split control strategies in a versatile hardware-in-the-loop laboratory test bench for hybrid electric vehicles equipped with electrical variable transmission," *Appl. Sci.*, vol. 10, no. 12, p. 4253, Jun. 2020.

[5] A. Ali, K. Mahmoud, and M. Lehtonen, "Optimal planning of inverter-based renewable energy sources towards autonomous microgrids accommodating electric vehicle charging stations," *IET Gener., Transmiss. Distrib.*, vol. 16, no. 2, pp. 219–232, Jan. 2022.

[6] A. Ali, K. Mahmoud, and M. Lehtonen, "Optimization of photovoltaic and wind generation systems for autonomous microgrids with PEV-parking lots," *IEEE Syst. J.*, vol. 16, no. 2, pp. 3260–3271, Jun. 2022.

[7] O. Ouramdane, E. Elbouchikhi, Y. Amirat, and E. Sedgh Gooya, "Optimal sizing and energy management of microgrids with vehicle-to-grid technology: A critical review and future trends," *Energies*, vol. 14, no. 14, p. 4166, Jul. 2021.

[8] D. Xie, L. Yu, T. Jiang, and Y. Zou, "Distributed energy optimization for HVAC systems in University campus buildings," *IEEE Access*, vol. 6, pp. 59141–59151, 2018.

[9] I. Cvok, B. Škugor, and J. Deur, "Control trajectory optimisation and optimal control of an electric vehicle HVAC system for favourable efficiency and thermal comfort," *Optim. Eng.*, vol. 22, no. 1, pp. 83–102, 2020.

[10] R. Xiong, J. Cao, Q. Yu, H. He, and F. Sun, "Critical review on the battery state of charge estimation methods for electric vehicles," *IEEE Access*, vol. 6, pp. 1832–1843, 2018.

[11] M. Ye, X. Song, R. Xiong, and F. Sun, "A novel dynamic performance analysis and evaluation model of series-parallel connected battery pack for electric vehicles," *IEEE Access*, vol. 7, pp. 14256–14265, 2019.

[12] E. Samadani, R. Fraser, and M. Fowler, "Evaluation of air conditioning impact on the electric vehicle range and li-ion battery life," in *Proc. SAE World Congr. Exhib.*, Apr. 2014, pp. 3–5, doi: https://doi.org/10.4271/2014-01-1853.

[13] *NREL Works to Increase Electric Vehicle Efficiency Through Enhanced Thermal Management*. Accessed: Jul. 18, 2018. [Online]. Available: https://www.nrel.gov/docs/fy14osti/62241.pdf

[14] D. Jefferies, T. Ly, A. Kunith, and D. Göhlich, *Energiebedarf Verschiedener Klimatisierungssysteme Für Elektro-Linienbusse*. Dresden, Germany: Deutsche Kälte-und Klimatagung, 2015.

[15] *MAN Bus A37: HVAC Analysis & Benchmark With Theseus-Fe*. Accessed: 2013. [Online]. Available: https://www.theseus-fe.com/ths_content/publications/slides/20130819_slides_man-bus-a37_hvac-analysis-and-benchmark-with-theseus-fe_en.pdf

[16] A. Patil, M. Radle, B. Shome, and S. Ramachandran, "One-dimensional solar heat load simulation model for a parked car," SAE Tech. Paper 2015-01-0356, 2015, doi: 10.4271/2015-01-0356.

[17] Y. Zhang *et al.*, "Cabin thermal comfort simulation of truck based on CFD," SAE Tech. Paper 2015-01-0344, 2015, doi: 10.4271/2015-01-0344.

[18] A. Kusiak, M. Li, and F. Tang, "Modeling and optimization of HVAC energy consumption," *Appl. Energy*, vol. 87, no. 10, pp. 3092–3102, 2010.

[19] L. Perez-Lombard, J. Ortiz, and I. R. Maestre, "The map of energy flow in HVAC systems," *Appl. Energy*, vol. 88, no. 12, pp. 5020–5031, Dec. 2011.

[20] J. Vepsäläinen, K. Otto, A. Lajunen, and K. Tammi, "Computationally efficient model for energy demand prediction of electric city bus in varying operating conditions," *Energy*, vol. 169, pp. 433–443, Feb. 2019.

[21] I. Ullah, K. Liu, T. Yamamoto, M. Zahid, and A. Jamal, "Electric vehicle energy consumption prediction using stacked generalization: An ensemble learning approach," *Int. J. Green Energy*, vol. 18, no. 9, pp. 896–909, Jul. 2021.

[22] T. M. Tumas, B. Maniam, M. Mahajan, G. Anand, and N. Jain, "E-thermal: A vehicle-level hvac/ptc simulation tool," SAE, Warrendale, PA, USA, Tech. Rep., 2004.

[23] Y. Bai and Q. Bai, "Heat transfer and thermal insulation," in *Subsea Engineering Handbook*, 2nd ed., Y. Bai and Q. Bai, Eds. Boston, MA, USA: Gulf Professional Publishing, 2019, pp. 363–408.

[24] M. Kind, H. Martin, P. Stephan, W. Roetzel, B. Spang, and H. Müller-Steinhagen, "VDI heat atlas," German Eng. Soc. (VDI), Berlin, Germany, Tech. Rep., 2010, doi: 10.1007/978-3-540-77877-6.

[25] D. Annaratone, *Engineering Heat Transfer*. Cham, Switzerland: Springer, 2010.

[26] H. Walter and B. Epple, *Numerical Simulation of Power Plants and Firing Systems*. Cham, Switzerland: Springer, 2017.

[27] M. Kutz, *Mechanical Engineers' Handbook: Energy and Power*, vol. 4. Hoboken, NJ, USA: Wiley, 2015.

[28] H.-H. Braess and U. Seiffert, *Vieweg Handbuch Kraftfahrzeugtechnik*. Cham, Switzerland: Springer-Verlag, 2011.

AMBARISH KULKARNI (Member, IEEE) is currently a Senior Lecturer and the Director of Vehicle Engineering Team, Swinburne University of Technology (SUT), specializes in engineering informatics with focus on mobility, cognitive twins, and critical infrastructure applications. He is also an Adjunct and Honorary Professor at IIT Hyderabad and Sanjay Ghodawat University, India. His industry experience in product design combined with his knowledge on design tools encouraged the University to appoint him as the coordinator for product design engineering subjects, from 2014 to 2017. In 2017, he was promoted to a Senior Lecturer in computer aided engineering (CAE) and a Lead Academic Advisor for SUT's iconic formula society of automotive engineers (FSAE) race car team. He has been working on engineering informatics for enhancing process for human centered products using specialized digital technologies (virtual and augmented reality). He has demonstrated numerous local and international collaboration with various industry grants (e.g.: repeat customers) including the Australian Research Council (ARC) and the Cooperative Research Council (CRC). Through industry funding, he has managed seven research assistants (RA) and 22 Ph.D. candidates (11 completions in five years) focusing on mobility, manufacturing cognitive twins, and critical infrastructure.

He is a fellow of Engineers Australia and FSAE-Asia Pacific. His aim is to continuously empower Australian industries and students future ready with cutting edge technologies.

GERRIT BRANDES (Student Member, IEEE) received the B.Eng. degree in mechanical engineering from Ostfalia FH Wolfenbüttel, in 2016, and the M.Sc. degree in mechanical engineering from TU Braunschweig, in 2018.

He has been a Research Associate at the Institute of Automotive Engineering (IAE), TU Braunschweig, since 2018, and coordinates the lecture "Automotive Vibrations" at TU Braunschweig. His research interests include automotive drivetrain efficiency in simulation and testing, innovative powertrain validation methods, automotive NVH, and objectivities of customer perception.

AKHLAQUR RAHMAN (Senior Member, IEEE) received the B.Sc. degree in electrical and electronic engineering from American International University, Bangladesh, in 2012, and the Ph.D. degree in electrical engineering from the Swinburne University of Technology, Melbourne, Australia, in 2019.

He is currently the Course Coordinator and a Lecturer for Industrial Automation Discipline with the Engineering Institute of Technology (EIT). He has been teaching at a higher education level for eight years, since 2013. In 2021, he was elevated to "IEEE Senior Member." He has also been the Department Coordinator and a Lecturer at Uttara University, Dhaka, Bangladesh. His research interests include machine learning, artificial intelligence, cloud networked robotics, optimal decision-making, industrial automation, and the IoT. He has published several top journals, such as IEEE Transactions on Industrial Informatics, *Computer Networks*, IEEE Communications Surveys and Tutorials, IEEE Access, and *JSAN* (MDPI), while also attending several IEEE conferences (GLOBECOM, ISAECT, ICAMechS, and ISGT-Asia). Besides that, he is the Guest Editor of *JSAN* (MDPI) special issue on "Industrial Sensor Networks," and an Official Reviewer of *Robotics* (MDPI). He has also been part of the TPC for several conference, such as CCBD, IEEE Greentech, and IEEE ICAMechS.

SHUVA PAUL (Member, IEEE) received the B.S. degree in electrical and electronics engineering and the M.S. degree from American International University-Bangladesh, Dhaka, Bangladesh, in 2013 and 2015, respectively, and the Ph.D. degree in electrical engineering and computer science from South Dakota State University, Brookings, South Dakota, in 2019.

He is currently working as a Postdoctoral Fellow with the Georgia Institute of Technology. His current research interests include power system cybersecurity, collaborative autonomy, computational intelligence, reinforcement learning, game theory, and smart grid security for power transmission and distribution systems, events and anomaly detection, vulnerability and resilience assessment, and big data analytics. He has been actively involved in numerous conference, including the Session Chair of the IEEE EnergyTech, in 2013, and IEEE EIT, in 2019. He served as a Guest Editor for *Journal of Sensor and Actuator Networks*. He also serves as a Reviewer for many reputed conference, including IEEE PES General Meeting, SSCI, IJCNN, PECI, and ECCI, and journals including IEEE Transactions on Neural Networks and Learning Systems, IEEE Transactions on Smart Grid, *Neurocomputing*, IEEE Access, *IET The Journal of Engineering*, and *IET Cyber-Physical Systems: Theory & Applications*.